Numerical analysis of non-visous potential flows

Edgar Gago Carrillo

Polytechnic University of Catalonia, Barcelona, Spain
edgar.gago@upc.edu | edgargc.upc@gmail.com
November 1, 2020

Abstract — This report is aimed to provide the lecturer with a first approach to the computational fluid dynamics simulations field focusing on potential flows. In this report the analysis of three use cases will be analysed and the code structure and a brief theoretical analysis of the problems will be done.

1 Introduction

This report shows to the reader the application of the Potential Flow theory for three simple case of study. The objective is the understanding of the theory and how it is applied for developing a numerical analysis on this cases. In order to present the contents in a ordered and fluid way the report is divided in three main sections.

All three sections are directly focused on the application of the developed theory during the theory class lectures by applying it to three different cases in order to give a better understanding of the Potential Theory.

This sections keep the same structure, talking about the problem definition and how it has been discredited. Further-more, it shows the coding structure followed for the development of the problem and the results and conclusions obtained.

2 Code structure

The code structure followed in the development of this project can be seen on (Fig 1).

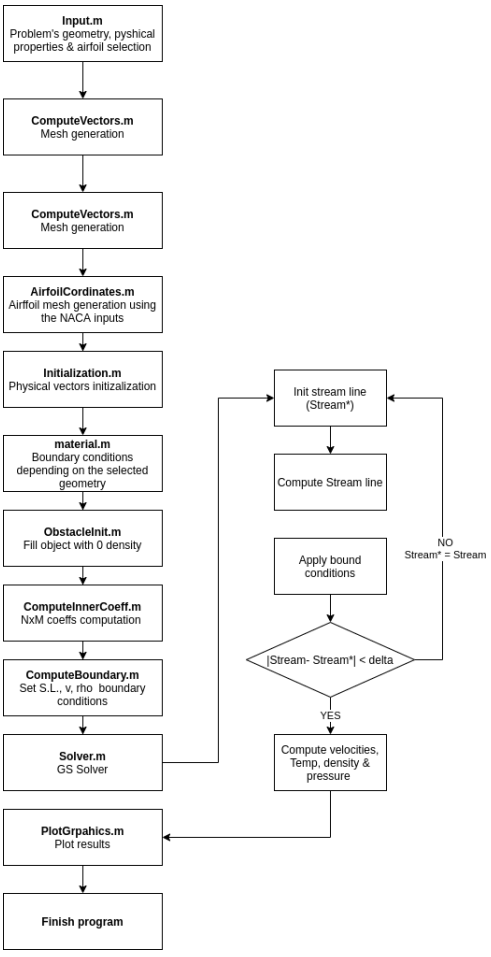

Figure 1: Program algorithm

As the the scheme is quite self explanatory, no further comments about it will be done. For a better resolution, the source of the algorithm structure can be found here: Algorithm source image. Note the bold text make reference to the scrips used in the code that can be found in the: Non-viscous

3 Theory discussion

This extended introduction is intended to provide the reader with a wider knowledge regarding the theory behind the project.
In this section the basis of the applied theory and how it is needed to work with the govern equations in order to develop a suitable numerical analysis. Since the objective is not to deepen into the numerical study the work is focused on the mathematical modeling and physical phenomena study of the problems presented.

3.1 Potential Flow

All the sciences of engineering need a compromise between reality and the needed simplifications for the mathematical calculations. The potential flow is a highly idealized theory used for modeling flows that match with the following assumptions:

- *Incompressibility.* The density and specific weight of the fluid is considered constant.
- *Irrotationality.* It implies a non-viscous fluid which particles move without rotation.

$$rot\,\overrightarrow{V} = 0 \tag{1}$$

- *Permanent Flow.* Which means that all the fluid properties and parameters are independent from time. [3]

The analysis of non-viscous regions is determined by the Euler Eq. 2.

$$\frac{\partial \rho}{\partial t} + \nabla \cdot (\rho \vec{v}) = 0 \tag{2a}$$

$$\frac{\partial \rho \vec{v}}{\partial t} + \nabla \cdot (\rho \vec{v}\vec{v}) = -\nabla p \tag{2b}$$

$$\frac{\partial E}{\partial t} + \nabla \cdot (E \vec{v}) = -\nabla \cdot (p \vec{v}) \tag{2c}$$

When it comes to solving the Euler equations, where the non-viscous regions can be considered irrational, two approaches will be considered:

- Mathematical formulation based on the stream function definition
- Mathematical formulation based on the velocity potential formulation. [2]

For developing this project is has been chosen the first approach. The stream function is defined by Eq. 3 for a steady 2D case which satisfies the mass conservation equation $\nabla \cdot (\rho \vec{v}) = 0$.

$$v_x = \frac{\rho_0}{\rho} \frac{\partial \phi}{\partial y} \tag{3a}$$

$$v_y = -\frac{\rho_0}{\rho} \frac{\partial \phi}{\partial x} \tag{3b}$$

Finally applying the equation for irrational flows it is possible to find:

$$\frac{\partial}{\partial x}\left(\frac{\rho_0}{\rho}\frac{\partial \phi}{\partial x}\right) + \frac{\partial}{\partial y}\left(\frac{\rho_0}{\rho}\frac{\partial \phi}{\partial y}\right) = 0 \tag{4}$$

Equation 4 is the one which defines the mathematical and physical principles involved in the resolution of the problem.

3.2 Numerical Analysis

3.2.1 Control-Volume Formulation

The basic idea of the control-volume formulation lends itself to direct physical interpretation. The calculation domain is divided into a number of non overlapping control volumes so that there is one control volume surrounding each grid point. Then it is needed to integrate the differential equation over each control volume. Piece-wise profile seen in Fig. 2 shows the variation of ϕ between their neighbour grid points used for evaluating the govern equations integrals resulting in a discretization equation that will contain the values of ϕ for a group of grid points.

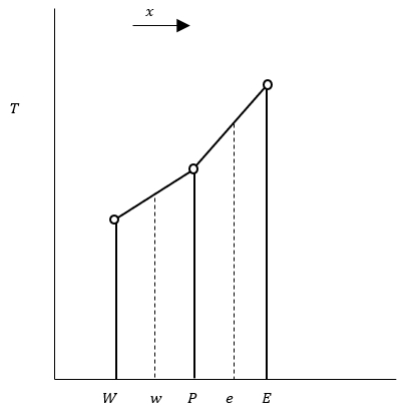

Figure 2: Piecewise - linear profile

The conservation equation obtained from the finite control volume study expresses its conservation principles for ϕ, just as the differential equation expresses it for an infinitesimal control volume. One of the most desirable features of this formulation is that the resulting solution would imply the integral conservation quantities such as mass, momentum and energy is exactly satisfied over any group of control volumes and over the whole calculation domain.

When it is needed to solve the discretization equation to obtain the grid-point values of ϕ, which are only needed to constitute the solution, without any explicit reference as to how ϕ varies between the grid points. The solution should only be dependent on the grid point values.

Grid-point scheme shown in the Fig.3 is going to be employed to derive the discretization equation. This scheme can be extended to two and three-dimensional situations, that is why it is only needed to describe it in this section. Grid point P has grid points W and E as neighbours, E denotes east $(+x)$ side and W west side $(-x)$. The dashed lines show the faces of the control volume denoted by letters e and w following the previous criterion.

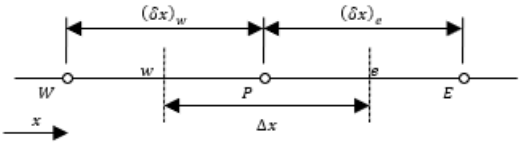

Figure 3: Grid-point scheme for one-dimensional problem

3.3 Equation Discretization

As it has been said, when the govern equation is obtained is is needed to discretize it. The discretization concepts lays in the idea of dividing the domain of study into different small interconnected pieces, each one of them governed by the discretized equation. Since each of the problems needed to be solved are considered irrotational, Stokes Theorem (Eq. 5)shows the path for obtaining the discretized equation.

$$\Gamma = \oint_C \overrightarrow{v} \cdot d\overrightarrow{l} \tag{5}$$

Due to the irrotationality the Circulation (Γ) is assumed to be zero. For a 2D case the integration of the velocity over the control volume faces gives the following expression:

$$\Gamma = v_{ye}\Delta y_P - v_{xn}\Delta x_P - v_{yw}\Delta y_P + v_{xs}\Delta x_P = 0 \quad (6)$$

Introducing the stream function definition the differentials in x and y directions are expressed as:

$$-\frac{\rho_0}{\rho_e}\frac{\psi_E - \psi_P}{d_{PE}}\Delta y_P - \frac{\rho_0}{\rho_n}\frac{\psi_N - \psi_P}{d_{PN}}\Delta x_P + \frac{\rho_0}{\rho_w}\frac{\psi_P - \psi_W}{d_{PW}}\Delta y_P + \frac{\rho_0}{\rho_s}\frac{\psi_P - \psi_S}{d_{PS}}\Delta x_P = 0 \quad (7)$$

Rearranging Eq. 7 terms is is obtained the coefficient form of the final discretization equation needed to solve the Potential Flow problem in the interior nodes volumes shown in Fig. 5.

$$a_P\psi_P = a_E\psi_E + a_W\psi_W + a_N\psi_N + a_S\psi_S + b_P \quad (8)$$

With coefficients,

$$a_E = \frac{\rho_0}{\rho_e}\frac{\Delta y_P}{d_{PE}} \quad (9a)$$

$$a_W = \frac{\rho_0}{\rho_w}\frac{\Delta y_P}{d_{PW}} \quad (9b)$$

$$a_N = \frac{\rho_0}{\rho_n}\frac{\Delta x_P}{d_{PN}} \quad (9c)$$

$$a_S = \frac{\rho_0}{\rho_s}\frac{\Delta x_P}{d_{PS}} \quad (9d)$$

$$a_P = a_E + a_W + a_N + a_S \quad (9e)$$

$$b_P = 0 \quad (9f)$$

3.4 Geometry Discretization

There are many possible ways for locating the control-volume but for the aim of this project only two different grids are explained. The description of each one will refer to a two-dimensional situation, although the concepts involved are applicable to one and three-dimensional situations.

3.4.1 Grid A: Faces located midway between the grid points

One of the most intuitive practises to construct the control volume is to place their faces *midway* between neighbouring grid points as seen in Fig.4. For building this grid to a 2-D plate grid points should be placed on its boundaries. Another observation is that the grid is nonuniform; the consequence of which is the grid point P does not lie at the geometric centre of the control volume.

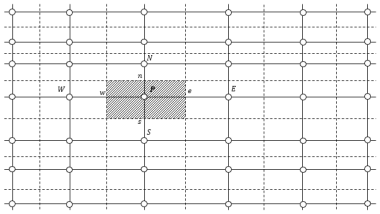

Figure 4: Location of control-volume faces - Grid A

3.4.2 Grid B: Grid points placed at the centres of the control-volumes

Another way to draw the grid is to draw the control-volume boundaries first and then place the grid point at the geometric centre of each control-volume. As it is seen in Fig.5 when the control volume sizes are non-uniform, their faces does not lie midway between the grid points.

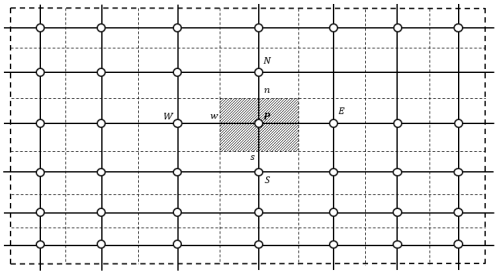

Figure 5: Location of control-volume faces - Grid B

The fact that the grid point P in Fig.4 may not be at the geometric centre of the control volume represents a disadvantage. In a heat conduction case, the temperature T_P cannot be observed as good representative value for the control volume in the calculation of the source term, the conductivity, and similar quantities [4]. Grid A also presents objections in the calculation of the heat fluxes at the control volume faces, taking grid point e in Fig.4, for example, it is seen that it is not at the centre of the control-volume face in which it lies. Thus, its assumed that the heat flux at e prevails over the entire face brings some inaccuracy.

Grid B does not have these problems because the point P lies at the centre of the control volume by definition and points such as e lies at the centre of their respective faces. One of the decisive advantages of Grid B is that the control volume turns out to be the basic unit of the discretization method, it is more convenient drawing the control-volume boundaries first and let the grid-point locations follow as consequence.

There are some advantages of Grid A over Grid B but the aforementioned advantages that Grid B represents over grid A makes to consider that the election of Grid B for the problem formulation is going to be the most suitable. It is needed to make additional considerations for the control volume near the boundaries of the domain. In the chosen case (Grid B) it is convenient to completely fill the calculation domain with regular control volumes and to place the boundary grid points on the faces of the near-boundary control volume faces. Figure 6 shows this arrangement of the Grid B where a typical boundary face i is located not between the boundary point B and the internal point I, it actually passes through the boundary point.

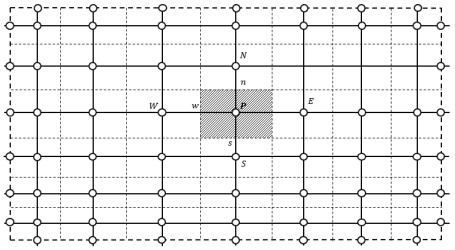

Figure 6: Boundary control volumes in Practice B

4 Flow inside a channel

The first case of study consists in solving a simple flow in a channel. Figure 12 shows a graphical representation of the real problem, which would consists in two flat plates with an air flow in between them.

As it is one of the most simple cases for studying the Potential Flow this case is a suitable first approach for modelling the fluid field. Table 1 and 2 show the geometrical parameters and physical properties needed for solving the problem.

Geometrical Property	L	H	N	M
Value	3	9	20	180

Table 1: Domain geometry discretization for Case 1

Table 2: Fluid of study (Air) physical properties for Case 1

$T(K)$	$P(Pa)$	$\rho(kg/m^3)$	ψ_0
300	100000	1.0595	3

γ	$R(J/kgK)$	$c_p(J/kgK)$	$v_0(m/s)$
1.394	287	$5/2 \cdot R$	4

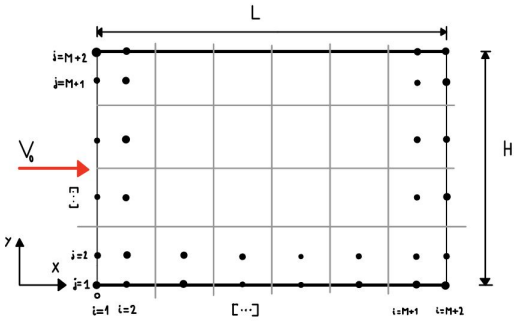

Figure 7: Problem definition and geometry discretization for Case 1

4.1 Boundary Conditions

For the numerical analysis and development of each case of study it is necessary to establish the meaning of boundary conditions. For the scope of this project the conditions described below are enough to model any of the phenomenons of study.

4.2 Dirichlet Boundary Condition

When solving ordinary or partial differential equations in the presence of a boundary, there needs to be a boundary condition on the solution. Dirichlet boundary conditions are a specification of the value that the solution takes itself on the boundaries of the domain.

$$\phi = Val \tag{10}$$

4.2.1 No-Slip Boundary Condition

The use of the no-slip condition illustrates well the use of scientific models and idealizations but more importantly, that condition gives us a realistic macroscopic approach to a realistic model. [1]

$$\phi = v; \quad Val = v_{wall}; \quad \rightarrow \quad v = v_{wall} \tag{11}$$

4.3 Neumann Boundary Condition

This condition when imposed on an ordinary or a partial differential equation specifies the derivative values of a solution over the boundary domain:

$$\frac{d\phi}{dn} = Val \tag{12}$$

Table 3 shows the conditions defined for solving this case of study.

Boundary	a_N	a_S	a_E	a_W	a_P	b_P	ψ_P
Top	0	0	0	0	1	0	$v_o \cdot H$
Bottom	0	0	0	0	1	0	0
Inlet	0	0	0	0	1	0	$v_0 \cdot y_P$
Outlet	0	0	0	1	a_W	$v_0 \cdot y_P$	ψ_W

Table 3: Boundary conditions for Case 1

4.4 Results

After having defined the boundary conditions applied to the projects it is possible to present and discuss the obtained solutions. The algorithm can be found on the (Fig.**??**) as it is the same for all the problems, also the function equations used each case are presented.

4.4.1 Verification

In order to verify the results validity it is needed to compare the obtained results with an already verified problem solution. As Figure 8 shows, the expected results consists in a uniform distribution of the potential field value along the horizontal direction of the flow. Each one of the streamline has a constant value of $v_0 \cdot y$.

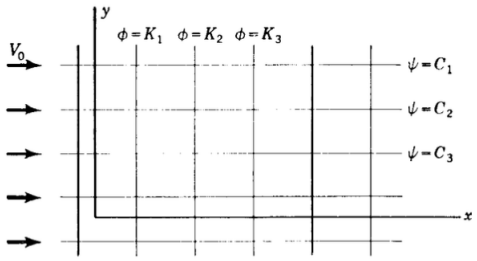

Figure 8: Flow net for uniform potential flow [3]

The following figure shows the behaviour of the developed code. It is seen that the the Stream Function streamlines correspond to the expected ones which would give the code the needed validation for the further computing of the velocity, pressure, temperature and density field.

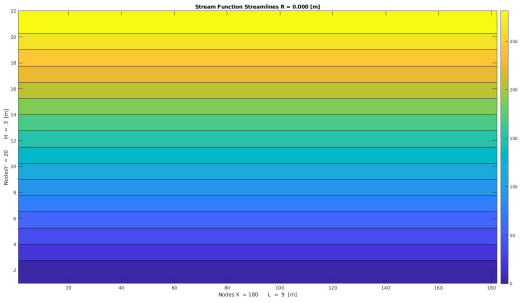

Figure 9: Stream Function streamlines for a 20x180 mesh in Case 1

4.4.2 Flow inside a channel

As the streamline representation has already been presented it is not going to be commented in this sub section.

Since the fluid of study is considered non-viscous as it was expected the velocity along the channel does not vary, taking as value the one introduced at the inlet condition. Figure 10 also shows the no-slip boundary condition placed at the solid boundaries of the domain of study.

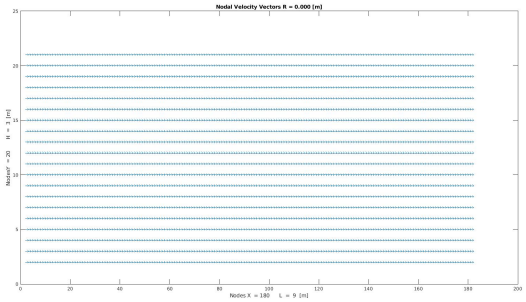

Figure 10: Nodal field for a 20x180 mesh in Case 1

The following Figures (Fig. 11 - **??**) show the expected solution for the temperature, density and pressure field. In order to save space neither the density nor the pressure graphics were printed as present the same result as the temperature. It can be seen clearly all the results remain constants trough the channel as expected.

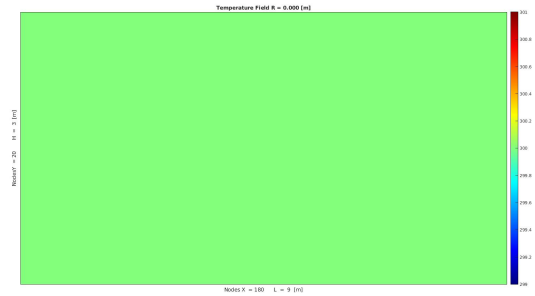

Figure 11: Temperature field for a 20x180 mesh in Case 1

5 Flow around a cylinder

This case of study consists in solving a simple flow in a channel for the study of how it interacts with simple objects such as a cylinder. Figure 12 shows a graphical representation of the real problem, which would consists in two flat plates with an air flow in between them with a cylinder placed in between. This case is an extension from the first one and both the geometry is the same but smaller but kepping the same ratio and the physical properties remain the same (Tab. 1) and (Tab.2)

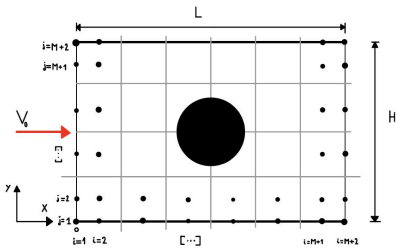

Figure 12: Problem definition and geometry discretization for Case 2

5.1 Boundary Conditions

Table 4 shows the conditions defined for solving this case of study.

Boundary	a_N	a_S	a_E	a_W	a_P	b_P	ψ_P
Top	0	0	0	0	1	0	$v_o \cdot H$
Bottom	0	0	0	0	1	0	0
Inlet	0	0	0	0	1	0	$v_0 \cdot y_P$
Outlet	0	0	0	1	a_W	$v_0 \cdot y_P$	ψ_W

Table 4: Boundary conditions for Case 2

5.2 Blocking - Off

The use of this methods is only needed when the analysis of the fluid field involves the interaction of solid-fluid regions. The constrain for setting its nature is based on where the centroid of the CV lays, if it is inside the solid region, it is considered as a solid and the same for fluid ones.

The treatment of the fluid CVs surrounding are the main point of this criteria. Taking the East node as an example it is known that its circulation is computed as

$$\Gamma_e \approx v_{ye}\Delta y_P = -\frac{\rho_0}{\rho_e}\frac{\partial \psi}{\partial x}\Delta y_P \tag{13}$$

In the case of solid-fluid interface the continuity of the ψ derivative is not clear, however it could be approximated as follows

$$v_{ye} = v_{ye}^- = v_{ye}^+ \tag{14}$$

$$v_{ye} = -\frac{\rho_0}{\rho_P}\frac{\psi_e - \psi_P}{d_{Pe}} = \\ = -\frac{\rho_0}{\rho_E}\frac{\psi_E - \psi_e}{d_{Ee}} \tag{15}$$

$$v_{ye} = -\frac{\rho_0}{\rho_e}\frac{\psi_E - \psi_P}{d_{PE}} \tag{16}$$

For computing ρ_e it is needed to be evaluated at the face of the solid-fluid boundary. For evaluating this term it is needed to compute the harmonic [1] mean between them.

5.3 Results

As it is expected, all the result show the proper behaviour. If we take a look at the first two figures (Fig. 13) (Fig.14) it is possible to see both of them are complementary. As it is natural, when velocity increases, pressure decreases. This fact can be clearly seen here, as the velocity it's accelerated at the top and bottom of the cylinder the pressure drops on both sides.

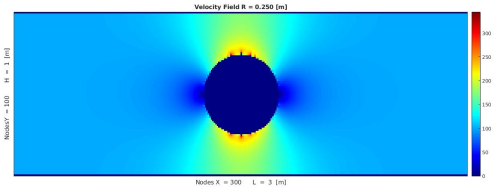

Figure 13: Velocity field in Case 2

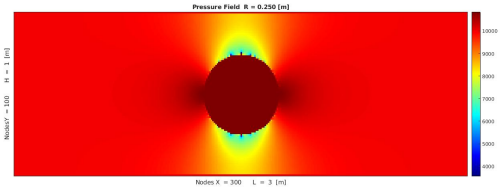

Figure 14: Pressure field in Case 2

Following the same logic if we take a look to temperature it should be linked to the previous ones. Moreover, in 15we can clearly see the pressure behaviour where a depression is formed on both vertical extremes of the cylinder and as the flow moves again

[1] More information regarding this calculation can be found here: Harmonic mean

the flow gains pressure recovering its original state.

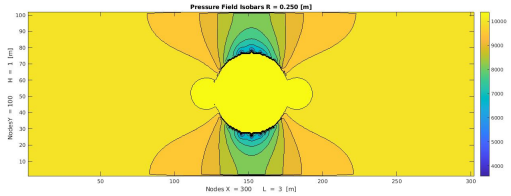

Figure 15: Isobars in Case 2

Finally, if we take a look at the streamline picture Fig. 16 we can clearly see haw these lines flow around the cylinder being compress by the extremes of the cylinder and the sides of the channel. As expected the flow velocity goes from 0 to 100. Again, in order to save space, some pictures are omitted as the behaviour can be applied to the temperature and the density as the velocity and the pressure show the expected behaviour.

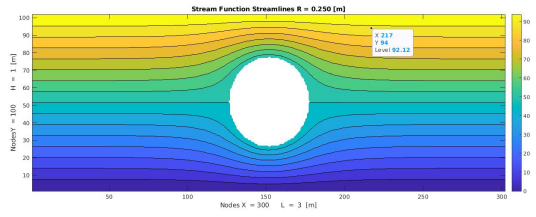

Figure 16: Stream lines field in Case 2

6 Flow around a NACAXXX

As an extra part for this project the computation of a flow around NACA 4 digits series code has been included. The additional code made for this project includes:

- Airfoil definition
- Airfoil positioning
- Airfoil stream lines constrains

Due to lack of time it has not been possible to properly developed this case study. In spite of that, a good enough simulation it has been possible to produce. The problems encountered where the following ones:

- The airfoil generation has to be placed in the middle of the channels and this generated a positioning problem. Easily solved after a careful review of the code.
- The hardest part was the mesh constraints that had to be generated in order to produce the streamlines around the fluid in order to be able to compute the fluid physical properties. After some time the constrains found almost approximated the full airfoils leaving outside an small part of it. After seeing the produced errors and reading about how to generate meshes around airfoils it was decided to try to compute some results the way it was and see whether the time would allow to make some improvements.

All physical and geometry are the the same as the ones used for the cylinder case.

6.1 Results

Regarding the results it has been found that they were quite accurate, even though the mesh discretization of the profile wasn't really optimised. The simulations were good enough in order to show the characteristics of the flow around an Airfoil. It was quite interesting to see how the flow behaved changing the NACA airfoil using the input script.

Probably the most interesting figure regarding this extra problem is the plot of the isobar field, this is because without computing the pressure coefficient distribution along the airfoil we can clearly see the how the flow is behaved around as expected, being accelerated on the upper part producing a decrease of the pressure. The other interesting part is that it can be seen

how the pressure drops on the on the maximum thickness point of the airfoil which is around 2m.

This result is expected as the the flow velocity show increase it's speed until the maximum thickness and after that should start decreasing. This point it is usually called center of pressure and it is used for aerodynamic calculations in order to be taken as a reference point for many problems.
To support the implementation of the proposed solution two more figures have been computed.

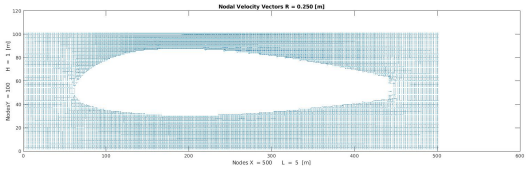

Figure 17: Nodal velocity field around the NACA foil

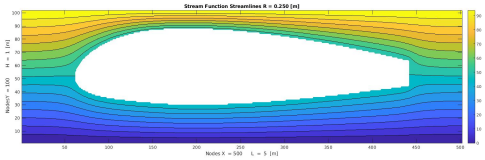

Figure 18: Streamlines around the NACA foil

It has not been considered necessary to produce more graphics as the ones provided (Fig. 17), (Fig.18) already show the expected behaviour of the flow around the airfoil which is to be accelerated on the upper side and properly follow the airfoil streamline.

It is expected to produce the following calculation from the presentation date to the final day of the subject in order to improve the quality of this last part:

- Optimize mesh airfoil conditions
- Produce a rotation matrix function in order to modify the angle of attack of the airfoil
- Compare the analytic solution of a single airfoils with theoretical solutions in order to test is feasibility

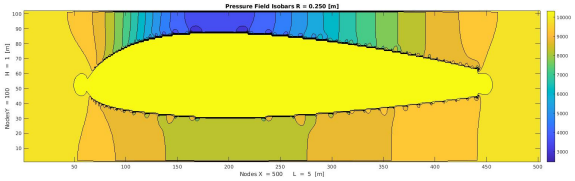

Figure 19: Caption

7 Computational cost analysis

Finally in order to briefly evaluate how the number of nodes affects the computational the following graphic has been created:

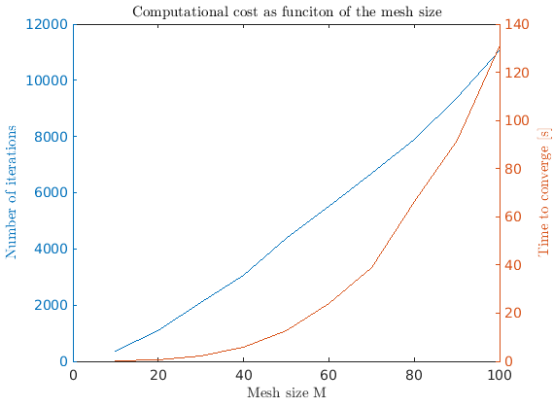

Figure 20: Computational cost

where it can be clearly see how the number of iterations it is affected lineally by the number of nodes or the size of the discretization. Meanwhile the computational time of the solver, which only takes into account the GS resolution, grows exponentially as the number of nodes increases.

The (Fig. 20 shows the important role supercomputers play in fluid dynamics. Because taking M = 40 the time to process it is around 6.0417s, meanwhile the for the

twice the number of nodes, the time to converge the GS solutions is 66.3629s, more than 10 times.

Finally, just mention the computational cost of the solver could be reduces using a different numerical solver such as the line-by-line or any other iterative method that could be faster in terms of convergence than the GS.

References

[1] A., M. *The no-slip condition of fluid dynamics. Academic Press.* Erkenntnis, 2004.

[2] CTTC. *Course on Numerical Methods in Heat Transfer and Fluid Dynamics. Non-Viscous Flows.* ESEIAAT.

[3] Shames, I. H. *Fluid Mechanics.* McGraw-Hill, 1995.

[4] V.Patankar, S. *Numerical Heat Transfer and Fluid Flow*, 1st ed. 1980.